Published by
NIGERIAN SOCIETY OF PHYSICAL SCIENCES
Available online @ https://journal.nsps.org.ng/index.php/jnsps

J. Nig. Soc. Phys. Sci. 3 (2021) 74–81

Journal of the Nigerian Society of Physical Sciences

Synthesis of SnO_2/CuO/SnO_2 Multi-layered Structure for Photoabsorption: Compositional and Some Interfacial Structural Studies

L. O. Animasahun[a,b,*], B. A. Taleatu[a], S. A. Adewinbi[a,c], H. S. Bolarinwa[b], A. Y. Fasasi[d]

[a]*Department of Physics and Engineering Physics, Obafemi Awolowo University, Ile Ife, Nigeria*
[b]*Department of Physics Electronics and Earth Sciences, Fountain University Osogbo, Nigeria*
[c]*Department of Physics, Osun State University, Osogbo, Nigeria*
[d]*Center for Energy Research and Development, Obafemi Awolowo University, Ile Ife, Nigeria*

Abstract

Many metal oxide heterostructures have been synthesized as mixed oxides or layered structures for photocatalytic, photodegradation of pollutants and light-harvesting applications. However, in the layered structures the effects of interfacial properties and composition have largely not been explored. Hence, the effects of interfacial mixing and diffusion of sandwiched thin CuO layer on optical absorption of as-deposited and heat-treated multi-layered structured SnO_2/CuO/SnO_2 films were studied. The RBS analysis of the as-deposited films showed the presence of a minute amount of Cu in the surface and bottom SnO_2 layers of the structure. We attributed this to inhomogeneous layer thickness evidenced by very low Sn/Cu atoms ratio of the CuO layer. However, the thermal treatment of the layered structure led to pronounced interlayer mixing and consequent formation of SnO_2-CuO solid solutions throughout the layered structure. The layer integrity of the inserted CuO of the as-deposited films was very high and the as-deposited structure was far more optically absorbing. However, the annealed structure showed lesser optical absorption because of the onset of interfacial mixing and improved crystallization. This reflected in the optical bandgap variations of the as-deposited and annealed multilayered structures. The significance of this result is that the multi-layered films possess band narrowing – evidence of increased photon absorption - making it a better candidate than pure SnO_2 oxide for photocatalysis, photodegradation and photodetection applications. It also pointed to the fact that attention must be paid to effects of heat treatments or annealing when inserting an absorbing layer into a photocatalyst or a material meant for photodegradation or any light-harvesting material.

DOI:10.46481/jnsps.2021.160

Keywords: Rutherford backscattering spectroscopy, thin films, interfacial mixing, optical absorption, photocatalysis, photodegradation

Article History :
Received: 26 January 2021
Received in revised form: 12 March 2021
Accepted for publication: 26 March 2021
Published: 29 May 2021

Communicated by: B. J. Falaye

1. Introduction

One of the attendant drawbacks of decades of global reliance on fossil energy sources is the environmental pollutions caused exploration processes and release of toxic wastes into the environment. Prominent among the various techniques that have been used in solving this problem is the use of metal oxides semiconductor heterostructures in photoabsorption and photocatalytic degradation of many pollutants [1-7] and detection of harmful gases [8-11]. Metal oxides heterostructures offer

*Corresponding author tel. no:
Email addresses: luqman.animasahun@gmail.com (L. O. Animasahun), afasasi@cerd.gov.ng (A. Y. Fasasi)

several advantages such as easy band engineering, improved charge carrier transport, increased electromagnetic photon absorption and overall better efficiencies over single oxides [1,4-5,12-15].

Many metal oxide heterostructures have been synthesized as mixed oxides or layered structures [2,5,6,13,15,16]. Besides, a lot of these heterostructures have been used for other applications such as electrocatalysts for fuel cells, an electron transporting layer in perovskite solar cells, photocatalyst for hydrogen productions [11,15,17,18]. However, despite these observed advantages, the confusion about the actual role of the added second oxides in photocatalysis or gas sensing in many heterostructures is yet to be cleared. The argument has been whether the added second oxide plays catalytic or carrier transport role or aids in photon absorption [17].

One way to gain insight into this problem is to know the relative positions of each constituent in the heterostructure. For instance, in gas sensing, an oxide that is not in contact with the analyte gas could not have performed a catalytic role. Hence, we have demonstrated in this work the use of Rutherford Backscattering Spectroscopy to investigate the composition, and thickness, and interfacial mixing of the inserted CuO layer in a SnO_2 /CuO/SnO_2 multi-layered film (Figure 1). RBS belongs to a cluster of techniques called ion beam analysis. It is a quantitative materials characterization technique that has been excellent for evaluating atomic densities of thin films and compositional depth profiling of blanket and multi-layered structures [19]. It is also capable of measuring quantitatively the interfacial mixing in multi-layered films. All of these parameters are central to the understanding and optimization of the properties of materials. Nevertheless, its application to investigate laterally inhomogeneous samples is chiefly unexplored.

Also, we investigated the effect of copper oxide insertion and interfacial diffusion on the optical bandgap structure of SnO_2. This is of importance to us because the optical bandgap determines to a very great extent the electromagnetic photon absorption properties of most materials. It predicts effectively whether a material will absorb only in the UV region or it will extend its absorption edge to the visible region of the e-m spectrum. This is of great importance in photocatalysis, photodegradation of pollutants and other light-harvesting applications. Besides, we examined the variations in the Urbach tail width as a result of thermal treatment to have an insight into the disorder, which could also affect optical absorption, in the multilayer film. We noted that several methods could be used in thickness determination of films [20]. However, most of these methods could not give compositional stoichiometry and depth profiling of the films. Our choice of SnO_2 as the base material is informed by its popularity in photodegradation and gas sensing applications [3,9,10,21-26]. Besides, because of its n-type semiconducting nature, CuO – a known p-type material was selected as the heterostructure pair.

We used a chemical spray pyrolysis method to obtain uniform and adherent films of the oxides. The spray pyrolysis process is a simple, robust and if properly controlled yields oxide films of high quality at rather low costs. Besides, it has the potential to produce thin layers of film on varieties of substrates.

2. Materials and Methods

Multi-layered films of SnO_2 and CuO on soda-lime glass substrate were deposited via spray pyrolysis technique. The spray solutions were prepared from analytical grade tin II chloride dihydrate salt, copper II nitrate trihydrate salt, ethanol and distilled water. 0.1 M clear solutions of $SnCl_2.{}_2H_2O$ and $Cu(NO_3)_2.3H_2O$ were prepared by dissolving appropriate mass of each salt in 50 ml of solvent and followed by vigorous stirring using a magnetic stirrer.

The soda-lime substrates were cleaned by washing in dilute hydrochloric acid, ethanol, acetone and distilled water in that order before drying. The deposition of the multi-layered films was carried out using the chemical spray pyrolysis technique. A schematic diagram of the setup is shown in Figure 2. In a typical deposition, the substrate temperature was maintained at 350 ± 5 ^{o}C while the nozzle-to-substrate distance and tilt angle of the spray gun was fixed at 23 cm and 45^o respectively. Each layer was deposited by spraying constant volume of the starting solutions for a constant number of passes (to and fro movement of the spray gun). The sequence of the layers is depicted in Figure 1. The first/bottom layer is SnO_2, followed by CuO and the topmost/surface SnO_2 layer. After deposition, the sample was annealed at temperatures between 400 - 550 ^{o}C for six hours in a tubular furnace.

The RBS experiment was performed using the 1.7 MeV Pelletron Tandem Accelerator at the Centre for Energy Research & Development, Obafemi Awolowo University, Ile-Ife, Nigeria. For this purpose, $4He^{2+}$ ion beam was used as the projectile ions. The scattering angle was 165^o and the resolution of the detector was 12 keV. During the process of acquiring the spectra data, the energy of the ion beam used was 2.2 MeV. All the measurements were performed at room temperature with current varying between 20 and 60 nA at a constant charge of 20 C. All the spectra were ?tted using Windows SIMNRA software for the estimation of composition and thickness of the ?lms. The surface morphology was studied using Scanning Electron Microscope at the University KwaZulu-Nata, Durban, South Africa. Crystal structures of the ?lms were determined through X-ray diffraction studies carried out with an X-ray Diffractometer model Bruker AXS D8 Advance. The optical properties were studied using UV–Visible – NIR Spectranet Ultraviolet spectrometer model EP2000.

3. Results and Discussions

3.1. Compositional Study

The simulations of RBS data were done using the Windows SIMNRA software. The result of the simulations gave the stoichiometric ratio of elements, compositions of layers and the film thickness of each sample. The RBS spectra are shown in figures (3) and the analysis presented in the table (1). Some important features could be inferred from the RBS analysis. The as-deposited sample has its inner/middle layer of CuO solidly intact with a minute amount of SnO_2. This is reflected in the Sn:Cu atomic ratio as shown in Table 1. This effect is also noticeable in the surface (SnO_2) and bottom (SnO_2) layers where

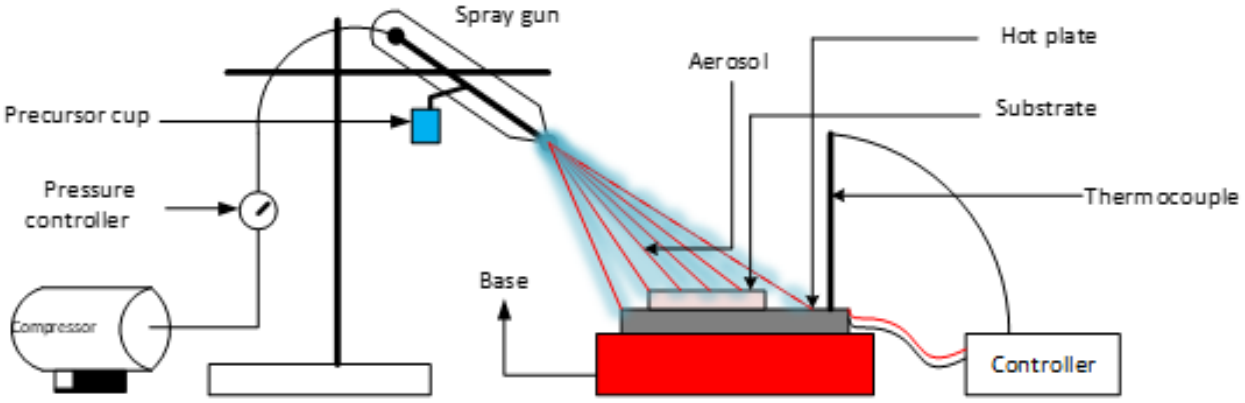

Figure 1. Spray pyrolysis set-up

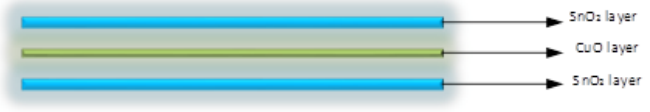

Figure 2. Multilayered SnO_2/CuO/SnO_2 films showing inter-diffusion

a small atomic per cent of Cu atoms is also present. The presence of the Sn atoms in the middle layer and Cu atoms in the surface and bottom layers could be attributed to a lot of factors – interfacial mixing, inhomogeneous layer thickness or surface roughness. Though these factors are somehow difficult to take into consideration in most IBA simulations, recent codes were able to incorporate these factors in RBS analysis [27]. In the heat-treated sample, however, the embedded middle CuO layer seems to have disappeared leaving behind multi-layered films which are composed of essentially solid solutions of the SnO_2 and CuO phases. This could be seen in the Sn:Cu ratio of the middle layer and the increase in the number of Cu atoms in the surface and bottom layers of the sample. It could be argued that this could also be attributed to any of the aforementioned factors - interfacial mixing, inhomogeneous layer thickness or surface roughness - however the obvious increase in the amounts indicated the effect of thermal treatment since both samples (as-deposited and annealed) were synthesized under the same conditions and with the same parameters, any observed difference in properties should be attributed to the effect of thermal treatment on the annealed sample. Besides, the annealed sample also showed an increase in thickness compared to the as-deposited one. This we attributed to the well-known behaviour of SnO_2 and most oxides whose grains grow in sizes when heated [28, 29].

The effects of these changes in compositions are pronounced in the optical absorption spectra of these samples. Also, it could result in the variations in the number of heterojunctions formed between the grains of the copper oxide and the tin oxide in the structure. The significance of this is that in explaining any observed effects in the applications of the layered films whether in gas sensing, energy harvesting or photocatalysis, attention must be paid to the possibility of compositional inhomogeneities in layers of the films. So, for instance, improved photon absorption could not possibly be the only justification/reason for improved photocatalytic behaviour for a surface that contains two catalytically active oxides. Summarily, the power of RBS in detecting a minute amount of interfacial diffusion and mixing is crucial in gaining insight into the understanding of observed effects and possible optimization of materials properties.

The surface morphology of the thin film structure of the annealed deposited SnO_2/CuO/SnO_2 multilayer is investigated using the SEM micrographs presented in Figure 4. To adequately assess its surface morphology, the micrographs are represented at various magnifications. The low magnification image shows networks of nanowalls that have grown with a nest-like structure. The nest-like structures were made up of a network of nanowalls that were non-uniform and interconnected. In terms of a vapour-solid model, the formation of such a specific structure has been explained [30]. Generally, precursor decomposition in spray pyrolysis involves four real-time important processes - residual solvent evaporation, droplet spreading, the formation of precipitate and vaporization, and salt decomposition – which precede and affect the formation of the film when aerosol droplets from the spray gun hit the surface of the heated substrate. The elevated temperature around the substrate caused the aerosol droplets to evaporate before reaching the substrate vicinity. Hence, the precipitate formation would occur as early as possible. As soon as the precipitates reached the heated substrate, they were converted to the vapour phase and then undergo a sequential heterogeneous reaction process

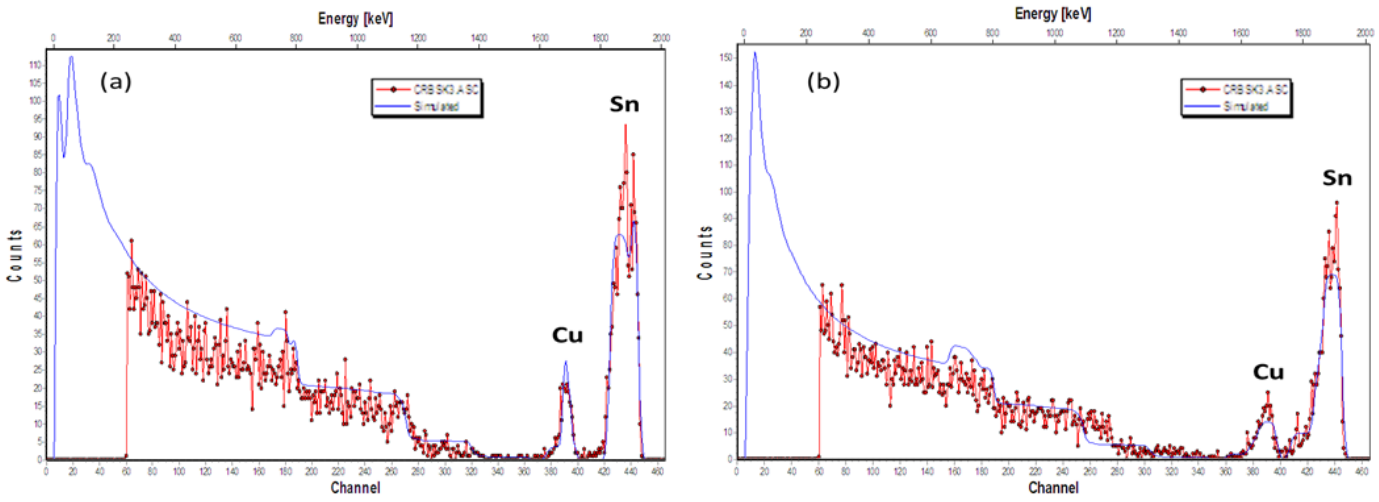

Figure 3. RBS Spectrum of (a) as-deposited and (b) annealed (at 500 ^{o}C) layered SnO_2/CuO/SnO_2 sample

Table 1. Results of the analysis of RBS data showing the compositions, layer thickness and Sn/Cu atomic ratios of the as-deposited and films annealed at 500 ^{0}C

Layers	Compositions As-deposited/Annealed@500 ^{0}C	Sn/Cu Ratios As-deposited/Annealed@500 ^{0}C	Thickness (nm) As-deposited/Annealed
Surface	$Sn_{0.12}0_{0.84}Cu_{0.04}$ / $Sn_{0.12}0_{0.81}Cu_{0.07}$	3.00/1.71	380/400
Middle	$Sn_{0.08}0_{0.40}Cu_{0.52}$ / $Sn_{0.07}0_{0.84}Cu_{0.09}$	0.15/0.88	140/230
Bottom	$Sn_{0.10}0_{0.88}Cu_{0.02}$ / $Sn_{0.08}0_{0.87}Cu_{0.05}$	5.00/1.60	500/550

starting with diffusion and adsorption of reactant molecules to the surface of the substrate. These are followed by surface diffusion and incorporation of molecules into the lattice and finally desorption and diffusion of the product molecules from the surface of the heated substrate. For that reason, during the beginning of the growth, a templating/seeding effect occurred directly on the substrate surface due to self-nucleation, following a high substrate temperature (360 ^{o}C) regime. After the self – nucleation of the seeds, heterogeneous nucleation and energy of the product molecules favoured the arrangement of product molecules into the observed nest – like morphology. The high density of both SnO_2 and CuO nuclei on the substrate surface easily coalesced into the growth of SnO_2/CuO/SnO_2 nanostructures during the SnO_2/CuO/SnO_2 nucleation and growth phase. At higher magnification Figure 4(b), interaction between each interface of the films is suspected. For our SnO_2/CuO/SnO_2 structure networks, the nanowall heights and widths have been found to be in the submicron region. Our parameters led to a classical CVD – like process that has been known to yield high sticking probability and quality films.

3.2. *X-ray Diffraction Analysis*

The X-ray diffraction patterns of the samples (shown in Figure 5) were studied to confirm the crystallinity of the samples and investigate the crystal structures of the as-deposited and heat-treated samples. The analysis of dominant peaks using Scherrer's formula confirmed the presence of polycrystalline SnO_2 and CuO phases. The SnO_2 is tetragonal rutile (cassiterite) and CuO is tenorite in nature according to crystallography open database (COD) reference entry no: 96-100-0063 and entry no: 96-101-1195, respectively [13,26]. Besides the increased intensities in the peaks of the annealed sample which implies improved crystallization, the XRD experiment did not reveal any new phases of the oxides even after the heat treatments. The orientation of the dominant peak remained the same indicating that the film is textured and corroborating our assertion that the annealing of the multi-layered films only led to interlayer mixing and diffusion of the oxides rather than the formation of a new chemical compound. Moreover, the positions of the peaks also agreed well with other reported works [31-33].

3.3. *Films' Optical Transmittance and Band Gaps*

The transmittance data obtained from the UV – Vis spectrophotometer at the CERD were analyzed to investigate the samples' optical energy band structures. The transmittance and Tauc's plots showing the bandgap determination and the effect of annealing temperature are presented in Figures 5(a and b). Figure 5(a) presents the normalized transmittance of the as-deposited and annealed multi-layered films. The as-deposited film was far more absorbing over the visible region than any of the annealed films. This could be attributed to the high transmittance of SnO_2 and the absorbing nature of CuO. When the film has not been annealed, the copper layer absorbed the transmitted light by the SnO_2 layer because the diffusion of the CuO in SnO_2 is still low. However, after the film was annealed the films become less absorbing because of improved crystallization and onset of diffusion of the absorbing CuO atoms in the

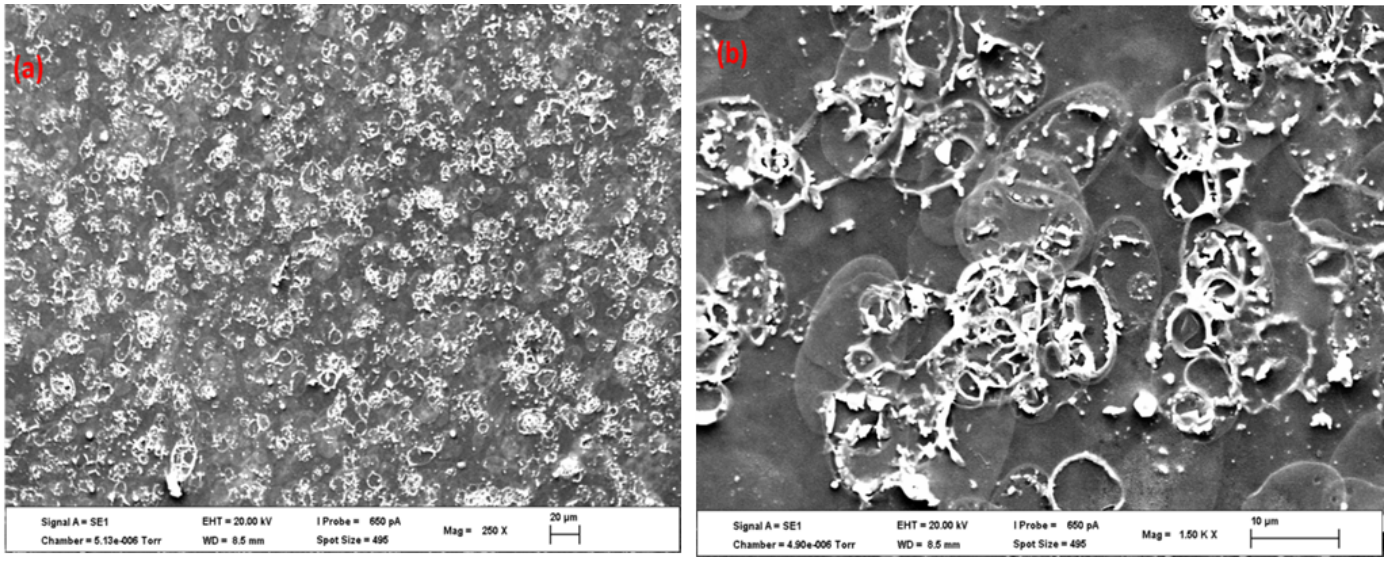

Figure 4. SEM micrographs showing surface features of annealed layered SnO_2/CuO/SnO_2

Table 2. Estimated values of optical bandgap and sub-bandgap

Sample	Optical bandgap (eV)	Urbach Energy E_u (eV)
As-deposited	2.75	1.37
Annealed @ 400 ^{o}C	3.45	1.92
Annealed @ 450 ^{o}C	3.47	1.92
Annealed @ 500 ^{o}C	3.49	1.76

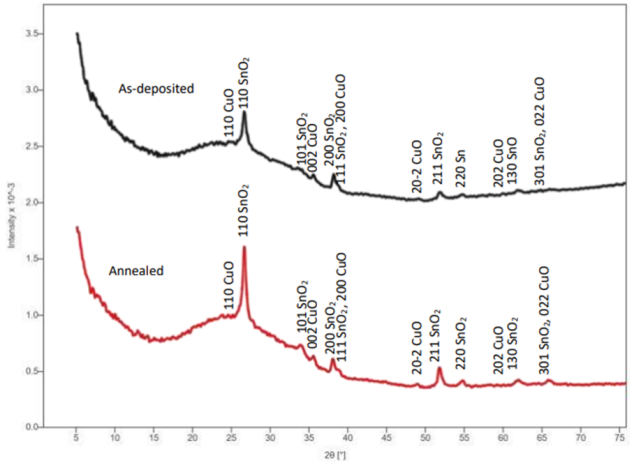

Figure 5. XRD pattern of layered SnO_2/CuO/SnO_2

SnO_2 matrix. In addition, adsorbed surface impurities which could have emanated from the deposition process, hinders the transition of light beam and might have been wiped off as a result of the heat treatments. This consequently reduces the absorption effect. The absorption coefficient α was generated from equation (1) using the transmittance data (assuming the films' reflectance is negligible) and film thicknesses obtained from the RBS analyses.

$$\alpha = \frac{1}{d} ln \frac{1}{T} \tag{1}$$

where d is the film thickness and T is the normalized transmittance. Optical energy band gaps for allowed direct and indirect transition were evaluated using the Tauc's relation in equation (2) assuming that the valence band and the conduction band are parabolic.

$$(\alpha h\upsilon)^{1/n} = A\left(h\upsilon - E_g\right) \tag{2}$$

where $h\upsilon$ is the photon energy, n is a power factor that determines the nature of transition, A is a band tail constant and E_g is the optical bandgap. n will take values of 1/2, 3/2, 2 and 3 for direct allowed, direct forbidden, indirect allowed and indirect forbidden transition respectively.

Tauc's method of plotting $(\alpha h\upsilon)^{1/n}$ against $h\upsilon$ was adopted to evaluate our deposited films' optical band gaps. The linear section of the resulting curve was then extrapolated to the photon energy, $h\upsilon$ axis which then gives the bandgap energy, E_g value. The plots are presented in Figure 5(b) and the films' estimated optical band gaps values are reported in Table 2. The results revealed the increase in the bandgap of the annealed film compared to the as-deposited film reflecting the observed features of the transmittance spectra. Also, in Figure 5(c), it was observed that there is a wide disparity (increase) between the bandgap of the as-deposited film and the film annealed at 400 ^{o}C. However, beyond 400 ^{o}C the multi-layered films showed a very negligible change in bandgap up to maximum annealing temperature of 550 ^{o}C. Of particular importance to us is the behaviour of the layered films compared to the well-known properties of pure SnO_2. For all values of annealing temperature

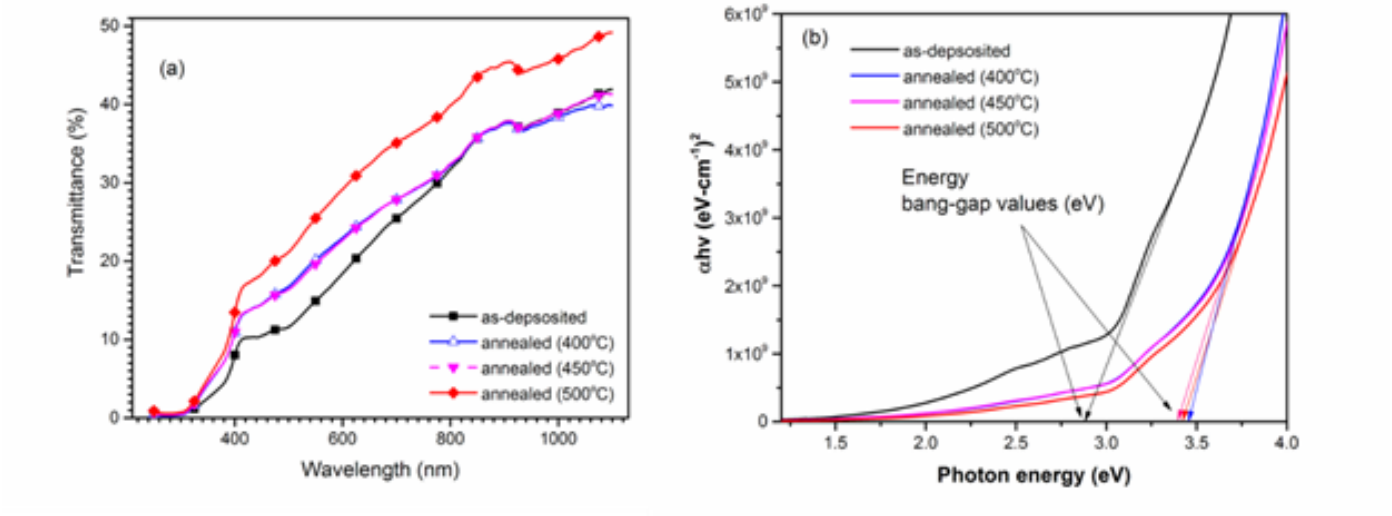

Figure 6. Figure 6: Plots showing (a) transmittance versus wavelength and (b) Tauc's plot for optical bandgap estimation

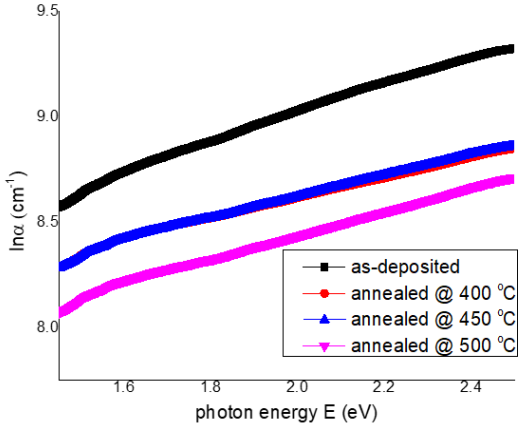

Figure 7. Plot for estimation of sub-bandgap (Urbach energy)

used, there was bandgap narrowing compared to the reported values between 3.5 – 4.0 eV [34,35] for pure SnO_2 even though the annealed films displayed higher band energies. This is evident that our deposited samples exhibit direct allowed photon energy transition. It also corroborates our earlier result showing that annealing has led to increased transmittance as a result of diffusion and/or mixing of the absorbing copper oxide layer and better crystallization. Incidentally, the optical bandgaps of the annealed layered films also coincide with the reported values for the copper doped tin oxide and SnO_2-CuO mixed or composite oxides. This corroborated the RBS analysis that after the heat treatment, the layers of the films essentially become mixed or solid solutions of the two constituent oxides. Band narrowing in the multi-layered film can be attributed to its increased photon absorption making it a better candidate than single layer SnO_2 for photocatalysis, photodegradation and photodetection applications. Our results also demonstrated the influence of heat treatments on the material's properties suitable for these applications. The thermal treatment led to decreased photon absorption compared to the as-deposited film as evidenced in bandgap behaviour. This would have profound effect on the photocatalysis and photodegradation ability of the multilayered films. Hence, in designing multilayered structures for light absorption applications, optimum annealing temperature should be chosen such that integrity of each layer would be maintained with little or less interfacial diffusion or mixing.

3.4. Urbach Energy

While it is has been established that optical bandgap gives fundamental pieces of information about band to band absorption properties of materials. However, beyond the lower limit value of bandgap, the structural characteristics of a material such as lattice distortions or disorder are capable of producing extended localized states in the energy gap of such materials leading to sub-bandgap absorption edge commonly called Urbach energy, E_u. In this lower photon energy range, the spectral dependence of the absorption edge follows the empirical Urbach rule given by equation (3) [1,33] where α_o and E_c are material constants, E is the photon energy and E_u denotes the width of the tail of localized states in the bandgap (Urbach energy)

$$\propto (E) = \alpha_o \exp\left(\frac{E - E_c}{E_u}\right) \tag{3}$$

The Urbach energy E_u was estimated by calculating the inverse of the slope of the linear fit obtained by plotting ln(α) against the photon energy E. The graphs are shown in Figure 7 and the results are presented in Table 2. Urbach energy can be seen as a measure of the energetic sharpness of the optical band edge. Usually, lower values of E_u suggest a high structural quality film or material which also indicates good electronic properties such as high carrier mobility [33]. As shown in Table 2,

the sub-bandgap for all the films was small indicating the good quality of the films. But most importantly the values of the Urbach energy also justify the RBS results that annealing the multi-layered films led to solid-state diffusion in their structure and consequently lattice disorder which resulted in the slight increase in the Urbach energies of the annealed. Though one would expect that annealing the film should lead to improving crystallization and better organization of the lattice and therefore lower Urbach energy, it seems the effect interlayer mixing dominated that of the crystallization and hence the increase in Urbach energy.

4. Conclusion

The thickness and composition of multi-layered SnO_2 /CuO /SnO_2 composite thin films were investigated using the RBS method. The RBS analysis of the films showed that the copper oxide layer in between the two SnO_2 diffused into the tin oxide matrix after annealing with minute amount reaching the surface layer and that the annealed sets of the same composition increased in thickness compared with the as-deposited sample. The bandgap for the as-deposited and annealed films was evaluated. It was discovered that copper oxide addition led to band narrowing and indirect band type as against the direct band type of tin IV oxide. This work gave the evidence of the suitability of copper oxide in narrowing the bandgap of tin oxide which is necessary for visible light photocatalysis and light-harvesting applications. It also demonstrated the applicability of the RBS in the study of solid-state diffusion in semiconductor materials.

Acknowledgments

We thank the anonymous referees for the positive enlightening comments and suggestions, which have greatly helped us in making improvements to this paper.

References

[1] S. A. Adewinbi, B. A. Taleatu, R. A. Busari, O. E. Adewumi, E. Omotoso, K. O. Oyedotun & N. Manyala. "Preparation and Surface Characterization of Nanostructured MoO_3/CoxOy and V_2O_5/CoxOy Interfacial Layers as Transparent Oxide Structures for Photoabsorption", Journal of Electronic Materials **49** (2020) 3837.

[2] . O. Animasahun, B. A. Taleatu, H. S. Bolarinwa, A. I. Egunjobi, A. Y. Fasasi, M.A Eleruja "Investigation of the Optical and Dielectric Behaviour of SnO_2-CuO Mixed Oxides Thin Films", Nigerian. Journal of. Pure & Appllied. Science **33** (2020) 3788.

[3] . T. Uddin, Y. Nicolas, C. Olivier, T. Toupance, L. Servant, M. M. Müller & W. Jaegermann, "Nanostructured SnO_2–ZnO Heterojunction Photocatalysts Showing Enhanced Photocatalytic Activity for the Degradation of Organic Dyes", Inorganic chemistry **51** (2012) 7764.

[4] . Ahmad & K. Majid, "Enhanced Visible Light-driven Photocatalytic Activity of CdO–Graphene Oxide Heterostructures for the Degradation of Organic Pollutants", New Journal of Chemistry **42** (2018) 3246.

[5] . K. Lakhera, A. Watts, H. Y. Hafeez, & B. Neppolian, "Interparticle Double Charge Transfer Mechanism of Heterojunction α-Fe_2O_3/Cu_2O Mixed Oxide Catalysts and its Visible-light Photocatalytic Activity", Catalysis Today **300** (2018) 58.

[6] . Elhalil, R. Elmoubarki, M. Farnane, A. Machrouhi, M. Sadiq, F. Z. Mahjoubi, & N. Barka, "Photocatalytic Degradation of Caffeine as a Model Pharmaceutical Pollutant on Mg-doped ZnO-Al_2O_3 Heterostructure", Environmental Nanotechnology, Monitoring & Management **10** (2018) 63.

[7] . Zhao, W. Ma, C. Chen, J. Zhao, & Z. Shuai, "Efficient Degradation of Toxic Organic Pollutants with Ni_2O_3/TiO_2-x B x under Visible Irradiation", Journal of the American Chemical Society **126** (2004) 4782.

[8] . Wang, L. Yin, L. Zhang, D. Xiang, & R. Gao, "Metal Oxide Gas Sensors: Sensitivity and Influencing Factors", Sensors **10** (2010) 2088.

[9] . W. Choi, A. Katoch, J. Zhang & S.S. Kim, "Electrospun nanofibers of CuO SnO_2 Nanocomposite as Semiconductor Gas Sensors for H_2S Detection", Sensors and Actuators B: Chemical **176** (2013) 585.

[10] . Chowdhuri, V. Gupta, K. Sreenivas, R. Kumar, S. Mozumdar, & P. K. Patanjali, "Response Speed of SnO_2-Based H_2S Gas Sensors with CuO Nanoparticles", Applied Physics Letters **84** (2004) 1180

[11] . T. Uddin, O. Babot, L. Thomas, C. Olivier, M. Redaelli, M. D'Arienzo & T. Toupance, "New Insights into the Photocatalytic Properties of RuO_2/TiO_2 Mesoporous Heterostructures for Hydrogen Production and Organic Pollutant photodecomposition", The Journal of Physical Chemistry C **119** (2015) 7006.

[12] . K. Dutta, S. K. Mehetor & N. Pradhan, "Metal Semiconductor Heterostructures for Photocatalytic Conversion of Light Energy", The Journal of Physical Chemistry Letters **6** (2015) 936

[13] . Pal, S. Maiti, U. N. Maiti & K. K. Chattopadhyay, "Low-temperature Solution-Processed ZnO/CuO Heterojunction Photocatalyst for Visible Light-Induced Photo-Degradation of Organic Pollutants", CrystEngComm **17** (2015) 1464.

[14] . Li & N. Chopra, "Structural Evolution of Cobalt Oxide–Tungsten Oxide Nanowire Heterostructures for Photocatalysis", Journal of Catalysis **329** (2015) 514.

[15] . Mahmood, B. S. Swain, A. R. Kirmani & A. Amassian, "Highly Efficient Perovskite Solar Cells Based on a Nanostructured WO_3–TiO_2 Core-Shell Electron Transporting Material", Journal of Materials Chemistry A **3** (2015) 9051.

[16] . Kumar, G. Sharma, M. Naushad, A. Kumar, S. Kalia, C. Guo, C & G. T. Mola, "Facile Hetero-assembly of Superparamagnetic Fe_3O_4/$BiVO_4$ Stacked on Biochar for Solar Photo-degradation of Methylparaben and Pesticide Removal from Soil. Journal of Photochemistry and Photobiology A: Chemistry 337 (2017) 118.

[17] . Sinatra, A. P. LaGrow, W. Peng, A. R. Kirmani, A. Amassian, H. Idriss & O. M. Bakr, "An Au/Cu_2O–TiO_2 System for Photocatalytic Hydrogen Production. A pn-Junction Effect or a Simple Case of in Situ Reduction?", Journal of Catalysis **322** (2015) 109.

[18] . Yang, S. Wang, C. Jiang, Q. Lu, Z. Tang & X. Wang, "Controlled Synthesis of Hollow Co-Mo Mixed Oxide Nanostructures and their Electrocatalytic and Lithium Storage Properties", Chemistry of Materials **28** (2016) 2417.

[19] . Laricchiuta, W. Vandervorst, I. Vickridge, M. Mayer & J. Meersschaut, "Rutherford Backscattering Spectrometry Analysis of InGaAs Nanostructures", Journal of Vacuum Science & Technology A: Vacuum, Surfaces, and Films **37** (2019) 020601.

[20] . Sammelselg, J. Aarik, A. Aidla, A. Kasikov, E. Heikinheimo, M. Peussa,.& L. Niinist, "Composition and Thickness Determination of Thin Oxide Films: Comparison of Different Programs and Methods", Journal of Analytical Atomic Spectrometry **14** (1999) 523.

[21] . Lin, Y. Chen & J. Ma, "Gas Sensing of SnO_2 Nanocrystals Revisited: Developing Ultra-sensitive Sensors for Detecting the H_2S Leakage of Biogas", Scientific Reports **4** (2014) 6028.

[22] . A. Miller, S. D. Bakrania, C. Perez & M. S. Wooldridge, "Nanostructured Tin Dioxide Materials for Gas Sensor Applications", Functional Nanomaterials (2006) 453.

[23] . Solís-Casados, E. Vigueras-Santiago, S. Hernández-López & M. A. Camacho-López, "Characterization and photocatalytic performance of tin oxide", Industrial & Engineering Chemistry Research **48** (2009) 1249.

[24] . A. Mahmoud & O. A. Fouad, "Synthesis and Application of Zinc/Tin Oxide Nanostructures in Photocatalysis and Dye-Sensitized Solar Cells", Solar Energy Materials and Solar Cells **136** (2015) 38.

[25] . H. Navidpour, M. Fakhrzad, M. Tahari & S. Abbasi, "Novel Photocatalytic Coatings based on Tin Oxide Semiconductor", Surface Engineering **35** (2019) 216.

[26] . Keles, M. Yildirim, T. Öztürk & O. A. Yildirim, "Hydrothermally Synthesized UV Light Active Zinc Stannate: Tin Oxide (ZTO: SnO2) Nanocomposite Photocatalysts for Photocatalytic Applications", Materials Science in Semiconductor Processing **110** (2020) 104959.

[27] . P. Barradas, "Rutherford Backscattering Analysis of Thin Films and Superlattices with Roughness", Journal of Physics D: Applied Physics **34** (2001) 2109.

[28] . Batzill, & U. Diebold, "The Surface and Materials Science of Tin Oxide", Progress in Surface Science **79** (2005) 147.

[29] . R. Miller, S. A. Akbar & P. A. Morris, "Nanoscale Metal Oxide-based Heterojunctions for Gas Sensing: A Review", Sensors and Actuators B: Chemical **204** (2014) 250.

[30] . Laurenti, & V. Cauda, "Porous Zinc Oxide Thin Films: Synthesis Approaches and Applications", Coatings **8** (2018) 67.

[31] . Patil, D. Kajale, D. Chavan, N. Pawar, P. Ahire, S. Shine, et al., "Synthesis, Characterisation and Gas Sensing Performance of SnO2 Thin Films Prepared by Spray Pyrolysis", Bulletin of Materials Science **34** (2011) 1.

[32] . Chen, Q. Zhou, F. Wan & T. Gao, "Gas Sensing Properties and Mechanism of Nano-SnO2 Based Sensor for Hydrogen and Carbon Monoxide", Journal of Nanomaterials (2012) https://doi.org/10.1155/2012/612420

[33] . Batal, G. Nashed & F. Jneed, "Electrical Properties of Nanostructure Tin Oxide Thin Film Doped with Copper Prepared by Sol-Gel Method", Latin America Journal of Physics Education **6** (2012) 311.

[34] M. Ledinsky, T. Schönfeldová, J. Holovský, E. Aydin, Z. Hájková, L. Landová, & S. De Brune, "Temperature Dependence of the Urbach Energy in Lead Iodide Perovskites", The Journal of Physical Chemistry Letters **10** (2019) 1368.

[35] L. O. Animasahun, B. A. Taleatu, H. S. Bolarinwa, A. Y. Fasasi, M. A. Eleruja & E. I. Obinajunwa, "Spray Pyrolysis deposition and characterizations of dielectric SnO_2 thin films". Fountain Journal of Natural and Applied Sciences 8 (2019) 11.